


Range-separated hybrid density functionals made simple

Cite as: J. Chem. Phys. **150**, 201102 (2019); <https://doi.org/10.1063/1.5097164>

Submitted: 22 March 2019 . Accepted: 06 May 2019 . Published Online: 28 May 2019

Éric Brémond , Ángel José Pérez-Jiménez , Juan Carlos Sancho-García , and Carlo Adamo 

COLLECTIONS

Note: This paper is part of the JCP Emerging Investigators Special Collection.

 This paper was selected as an Editor's Pick



View Online



Export Citation



CrossMark

ARTICLES YOU MAY BE INTERESTED IN

[An alternative derivation of orbital-free density functional theory](#)

The Journal of Chemical Physics **150**, 204109 (2019); <https://doi.org/10.1063/1.5096405>

[Perspective: Computational chemistry software and its advancement as illustrated through three grand challenge cases for molecular science](#)

The Journal of Chemical Physics **149**, 180901 (2018); <https://doi.org/10.1063/1.5052551>

[Performance of new density functionals of nondynamic correlation on chemical properties](#)

The Journal of Chemical Physics **150**, 204101 (2019); <https://doi.org/10.1063/1.5082745>

Lock-in Amplifiers up to 600 MHz

starting at

\$6,210



Zurich
Instruments

Watch the Video



Range-separated hybrid density functionals made simple

Cite as: J. Chem. Phys. 150, 201102 (2019); doi: 10.1063/1.5097164

Submitted: 22 March 2019 • Accepted: 6 May 2019 •

Published Online: 28 May 2019



View Online



Export Citation



CrossMark

Éric Brémond,^{1,a)}  Ángel José Pérez-Jiménez,²  Juan Carlos Sancho-García,²  and Carlo Adamo^{3,4} 

AFFILIATIONS

¹ Université Paris Diderot, Sorbonne Paris Cité, ITODYS, UMR CNRS 7086, 15 rue J.-A. de Baïf, F-75013 Paris, France

² Departamento de Química Física, Universidad de Alicante, E-03080 Alicante, Spain

³ Chimie ParisTech, PSL Research University, CNRS, Institute of Chemistry for Life and Health Sciences (i-CLeHS), FRE 2027, F-75005 Paris, France

⁴ Institut Universitaire de France, 103 Boulevard Saint Michel, F-75005 Paris, France

Note: This paper is part of the JCP Emerging Investigators Special Collection.

^{a)} **Electronic mail:** eric.bremond@univ-paris-diderot.fr.

ABSTRACT

In this communication, we present a new and simple route to derive range-separated exchange (RSX) hybrid and double hybrid density functionals in a nonempirical fashion. In line with our previous developments [Brémond *et al.*, J. Chem. Theory Comput. **14**, 4052 (2018)], we show that by imposing an additional physical constraint to the exchange-correlation energy, i.e., by enforcing to reproduce the total energy of the hydrogen atom, we are able to generalize the nonempirical determination of the range-separation parameter to a family of RSX hybrid density functionals. The success of the resulting models is illustrated by an accurate modeling of several molecular systems and properties, like ionization potentials, particularly prone to the one- and many-electron self-interaction errors.

Published under license by AIP Publishing. <https://doi.org/10.1063/1.5097164>

Within the history of Kohn-Sham density-functional theory (KS-DFT),^{1,2} one of the major breakthroughs came in the 1990s with the development of hybrid density functionals.^{3,4} Formally justified by the “adiabatic connection” formula,⁵ a mix of a fraction of nonlocal exactlike exchange (EXX) with a pure semilocal density-functional approximation (DFA) led to a new family of expressions. The resulting global hybrids (GHs) (partially) cure spurious issues arising from the locality problem like the one-electron self-interaction error (SIE) and its extension to many-electron systems.^{6,7} Within this class of approximation, the exchange-correlation energy is decomposed such as

$$E_{xc}^{\text{GH}} = a_x E_x^{\text{EXX}} + (1 - a_x) E_x^{\text{DFA}} + E_c^{\text{DFA}}, \quad (1)$$

where a_x governs the fraction of EXX, and E_x^{DFA} and E_c^{DFA} denote the exchange and correlation energy terms, respectively, generally expressed at the generalized gradient approximation (GGA) level.

If GHs guarantee a systematic performance improvement with respect to semilocal density functionals^{8,9} and a successful modeling of a large number of ground- and excited-state properties,^{10,11} they still suffer from a density overdelocalization in the long-range (LR) regime. Instead of correctly behaving as $-r_{12}^{-1}$, $r_{12} = |\mathbf{r}_2 - \mathbf{r}_1|$ being the electron-electron distance, the asymptote of their exchange potential behaves instead as $-a_x r_{12}^{-1}$.¹² This drawback leads systematically to an underestimation of the energy properties of molecular systems such as ionization potentials (IPs),^{13,14} intramolecular/intermolecular charge-transfer excitations,¹⁵ or the dissociation of open-shell complexes.^{16,17}

As an alternative to GHs, successive models were revealed themselves or were specifically developed to circumvent the locality problem. A nonexhaustive list of some of them counts for the self-interaction correction (SIC),^{18,19} the orbital dependence,^{20–22} the merging between density- and wavefunction-based approaches,^{23,24} or the recent multiconfiguration pair-DFT (MC-PDFT).^{25,26} Thanks to a concomitant wide implementation and an excellent performance improvement, the range-separated

exchange (RSX) scheme^{27,28} remains among the most popular alternative to GHs. It consists in a physically sound solution to impose to the exchange potential a $-r_{12}^{-1}$ asymptotic behavior by splitting the Coulomb operator into a short-range and a long-range (SR and LR, respectively) term

$$\frac{1}{r_{12}} = \underbrace{\frac{1 - [\alpha + \beta \operatorname{erf}(\mu r_{12})]}{r_{12}}}_{\text{SR=short range}} + \underbrace{\frac{\alpha + \beta \operatorname{erf}(\mu r_{12})}{r_{12}}}_{\text{LR=long range}}. \quad (2)$$

The error function erf smoothly connects the SR to the LR part of the operator under the governance of a range-separation parameter μ , which is usually determined empirically.^{27–29} When the range separation transformation is applied to the exchange potential, it holds the correct asymptotic behavior. The RSX energy thus becomes

$$E_{x,\mu}^{\text{RSX}} = \alpha E_x^{\text{EXX}} + \beta E_{x,\mu}^{\text{EXX}} + (1 - \alpha) E_x^{\text{DFA}} - \beta E_{x,\mu}^{\text{DFA}}, \quad (3)$$

with α and $\alpha + \beta$ being, respectively, two combined parameters monitoring the full and LR contribution of EXX. By setting the latter combination to 1, i.e., $\alpha + \beta = 1$, the RSX energy recovers the correct asymptote in the LR regime. Moreover, to conserve a satisfactory behavior of a GH in the SR regime, Eq. (1) imposes the parameter α to be equal to a_x . The resulting RSX exchange-correction hybrid energy is written as

$$E_{xc,\mu}^{\text{RSX-H}} = E_{xc}^{\text{GH}} + (1 - a_x) E_{x,\mu}^{\text{EXX}} - (1 - a_x) E_{x,\mu}^{\text{DFA}}. \quad (4)$$

By using Eq. (4), numerous challenging applications were tackled in an accurate way. We especially mention some conceptually simple systems particularly prone to SIE such as cationic rare gas dimers in their dissociation limit³⁰ or more complex properties like bond-length alternations (BLAs) in conjugated chains^{31,32} and long through-space charge-transfer excitations.^{33,34} Beyond the hybrid approximation, the range separation was also combined with multideterminantal, or more generally post-Hartree-Fock, extensions of KS-DFT to successfully model weakly interacting molecular systems.^{35–38} However, the obtained results strongly depend on the value assigned to the range-separation parameter.

The parameter μ is homogeneous to the inverse of a distance, and it measures how fast the range separation switches from the SR to the LR regime. Since the first implementation of the RSX method, several schemes were proposed to determine it. Some of them focused on an empirical parameterization to minimize errors on general or specific energy properties.^{39–43} They led to values for μ lying typically between 0.2 and 0.5 bohr⁻¹. Others turned to a nonempirical, but system-dependent, way to tune μ : they are based on an optimally tuned (OT) procedure which aims at fulfilling Koopmans' theorem within the KS framework by enforcing the agreement between the IP and the negative value of the HOMO energy ($-\epsilon_{\text{HOMO}}$).⁴⁴ Despite its large success with respect to ground- and excited-state applications^{45–47} and its recent implementation in a self-consistent fashion (scOT),⁴⁸ this approach remains computationally expensive and prone to size-consistency-related issues.⁴⁹

Another way to estimate the range-separation parameter in a nonempirical fashion consists in imposing an additional physical constraint while deriving the density functional. With this aim, we

recently showed that by enforcing the exact treatment of the ground state energy of the hydrogen atom, we succeeded to derive the RSX extension of the quadratic-integrand double-hybrid (QIDH) model and thus a density functional free from any kind of empirical parameterization.⁵⁰ The resulting RSX-QIDH double hybrid takes up the challenge to (i) accurately estimate IPs of molecular systems by following Koopmans' theorem,¹⁸ (ii) (closely) remedy the locality issue through the helium cluster example,⁶ and (iii) accurately reproduce previous results for SIE-prone properties not at the expense of others.

Motivated by the excellent performance provided by the RSX-QIDH model, our goal in this communication is to show that our nonempirical scheme to determine μ is generalizable to the transformation of any kind of GH into its corresponding RSX-H density functional. For that, we select a panel composed by a set of the most popular nonempirical global and double hybrids, all of them built from the Perdew-Burke-Ernzerhof (PBE) semilocal approximation,⁵¹ and we demonstrate that by turning them into a nonempirical RSX hybrid or double hybrid, we are able to accurately model various energy properties particularly prone to SIE.

Among nonempirical density functionals, PBE,⁵¹ PBE0,^{52,53} PBE0-1/3,⁵⁴ PBE0-DH,⁵⁵ and PBE-QIDH²⁴ are among the most popular. All of them cast an increasing fraction of EXX spanning between 0 and ~69% with values of a_x assigned to 0, 1/4, 1/3, 1/2, and $3^{-1/3}$, respectively. Their evolution from the global to the RSX scheme corresponds to a transformation of their exchange-correlation energy from Eqs. (1)–(4), their range-separation parameter μ being determined by enforcing the RSX density functional to reproduce the exact energy of the hydrogen atom. More information about the definition of these density functionals is reported in Table SI of the [supplementary material](#).

Figure 1 depicts the evolution of μ as a function of the whole fraction of EXX a_x for the RSX hybrids and double hybrids investigated herein. Globally, we observe a linear decrease in μ while a_x increases. Such a behavior means that the larger the whole fraction

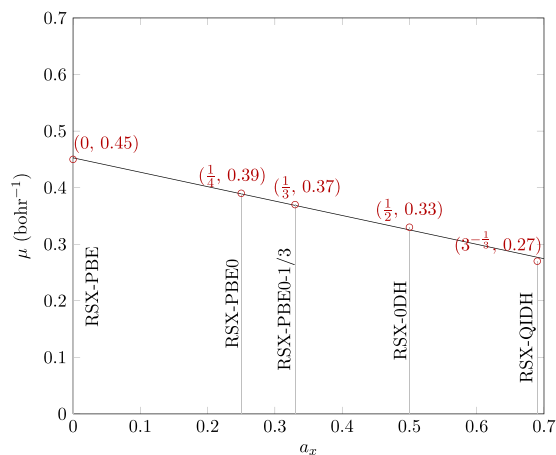


FIG. 1. Range-separation parameter μ (bohr⁻¹) determined to recover the energy of the hydrogen atom, as a function of the whole fraction of exactlike exchange a_x . More information about the definition of these density functionals is reported in Table SI of the [supplementary material](#).

of EXX is, the faster the switch from the SR semilocal term to the LR EXX one has to be, which can be viewed as a proof of the importance of the semilocal term of the density functional. In the domain $a_x \in [0, 3^{-1/3}]$, the linear relationship however has to be viewed as a rule of thumb since both double hybrids cast different fractions of semilocal correlation. As depicted by Fig. S1 of the [supplementary material](#), a quasilinear trend is only observed with the RSX-H model [Eq. (4)] when $a_x < 1/2$. Out of this domain, the relationship between a_x and μ is strictly nonlinear.

The values of the range separation parameter derived here are in line with the ones obtained by previous investigations based on an empirical parameterization with respect to ground- and/or excited-state properties. As a first example, Hirao *et al.* demonstrated that for the long-range corrected PBE (LC-PBE) density functional ($a_x = 0$), an optimal value of μ is 0.47 bohr^{-1} .⁵⁶ This value is to be compared with $\mu = 0.45 \text{ bohr}^{-1}$ in what we call here the RSX-PBE density functional. As another example, Herbert *et al.* showed that when $a_x = 0.25$, the fitting of μ with respect to a short selection of $\pi - \pi^*$ charge-transfer excitations gives $\mu = 0.35 \text{ bohr}^{-1}$.⁵⁷ Our RSX-PBE0 variant, which casts the same whole fraction of EXX, exhibits a slightly larger value of μ ($\mu = 0.41 \text{ bohr}^{-1}$).

To get an initial idea of the performance of the newly derived RSX hybrid and double-hybrid-based density functionals, we start by analyzing their accuracy to model IPs within the vertical and Koopmans' schemes [$\Delta_{\text{IP}}E = E(N-1) - E(N)$ or simply ΔSCF and $-\varepsilon_{\text{HOMO}}$, respectively]. The second-order perturbation theory term being computed *a posteriori*, the HOMO energies are evaluated from the self-consistent contribution to the total exchange-correlation expression. For that purpose, we select a set of 100 small organic molecules gathered in the GW100 database.⁵⁸ This not only has the advantage to be large enough, providing a fair statistical survey of the method performance, but also to be composed by references computed at the "gold standard" coupled-cluster

singles, doubles, and perturbative triples [CCSD(T)] level of theory,⁵⁹ avoiding inconsistencies introduced by experimental references.

Figure 2 reports the linear correlation, ruled by the coefficient of determination R^2 , between the vertical and Koopmans' estimates of the IP. Independent of the density functional, the RSX scheme improves systematically the linear agreement between both estimates with excellent values of R^2 . Compared with their corresponding non-RSX models, we find systematically larger R^2 values, remaining higher than 0.93 in all cases (i.e., for the PBE semilocal density functional). Regarding mean absolute deviations (MAD) with respect to the reference CCSD(T) IPs, the transformation from the global to the RSX scheme provides a quasisystematic performance improvement independent of the estimate approach, i.e., vertical IP (MAD_{IP}) or Koopmans' picture (MAD_{KS}). The largest MAD_{KS} decrease is found going from PBE to RSX-PBE (4.0 to 0.5 eV), while the smallest one is observed going from PBE-QIDH to RSX-QIDH (0.6 to 0.5 eV), the density functional casting an intermediate value of a_x providing an error decrease in between. The performance improvement with respect to MAD_{IP} is more moderate, the largest decrease being lower than 0.1 eV in the case of the PBE to RSX-PBE transformation. It is worth to note that MAD_{IP} is systematically half of MAD_{KS} for the whole family of density functionals derived from the RSX scheme.

A pragmatic way to judge SIE is the evaluation of the asymptotic dissociation energy of cationic diatomics, which should vanish for any well-behaved density functional. Indeed, the dissociation energy of the dihydrogen cation is considered as a proof of concept for the one-electron SIE. Table I reports these values for the panel of considered nonempirical RSX hybrids and double hybrids. The table also includes results from $\omega\text{B97X-D}$ ($a_x = 0.22$ and $\mu = 0.20 \text{ bohr}^{-1}$),³⁹ a parameterized RSX hybrid recognized for its excellent performance for various energy properties and taken thus

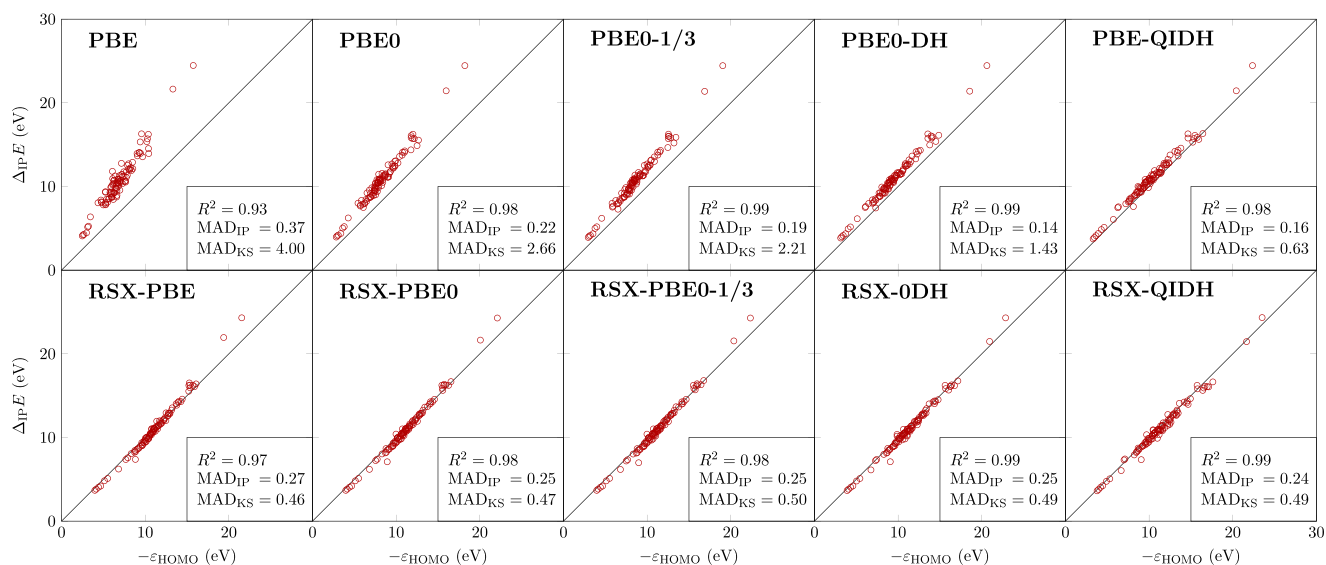


FIG. 2. Correlation diagrams comparing the ionization potential energies (eV) of 100 small molecules gathered into the GW100 dataset computed as the energy difference between the cationic and neutral systems, $\Delta_{\text{IP}}E$, and the energy of HOMO orbital $\varepsilon_{\text{HOMO}}$. All computations are performed with the def2-QZVP basis set.

TABLE I. Dissociation energy (kcal mol^{-1}) of selected diatomic radical cations X_2^+ computed at an interatomic distance of 100 \AA and the def2-QZVP basis set.

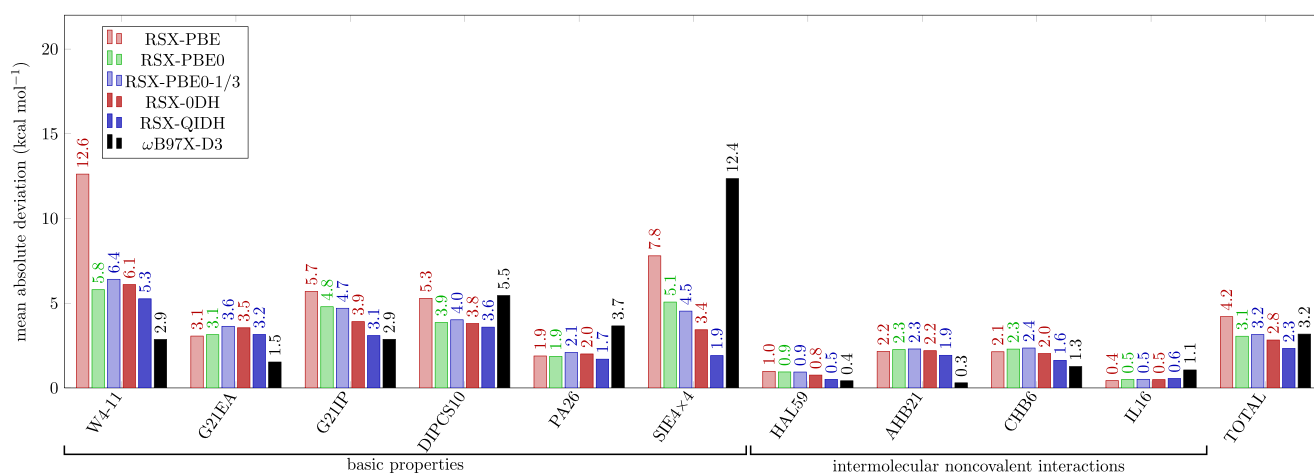
X_2^+	RSX-PBE	RSX-PBE0	RSX-PBE0-1/3	RSX-0DH	RSX-QIDH	ω B97X-D
H_2^+	-11.3	-10.6	-10.1	-8.9	-6.9	-28.3
He_2^+	-26.7	-21.2	-18.8	-14.5	-9.0	-47.5
Ne_2^+	-30.6	-19.0	-14.6	-10.9	-7.7	-41.9
Ar_2^+	-6.8	-4.4	-3.3	-3.1	-3.2	-21.5

here as reference. At 100 \AA , the dissociation energy of H_2^+ varies smoothly between -11.3 and $-6.9 \text{ kcal mol}^{-1}$ (RSX-PBE and RSX-QIDH, respectively) when the whole range of EXX increases. As a matter of comparison, ω B97X-D is outperformed by its new competitors and provides an absolute dissociation energy 4 times larger ($-28.3 \text{ kcal mol}^{-1}$). The same conclusions are inferred regarding rare gas cationic dimers such as He_2^+ , Ne_2^+ , and Ar_2^+ (Table I). The many-electron SIE is very low for the nonempirical RSX hybrid and double-hybrid family of density functionals. However, the absolute margin of improvement with respect to ω B97X-D is this time multiplied up to 7 times for RSX double hybrids on the example of the argon cation dimer (~ -3.0 vs $-21.5 \text{ kcal mol}^{-1}$). As a result, our nonempirical determination of μ provides again an excellent compromise to reduce SIE-prone properties.

To further validate the reliability of the newly derived RSX hybrids and double hybrids, we assess their performance on a selection of 10 subsets belonging to the very large GMTKN55 benchmark set.⁶⁰ Our selection counts for basic and intermolecular noncovalent molecular properties, some of them tending to be particularly prone to SIE (Fig. 3). Among basic properties, atomization energies probed through the W4-11 subset are generally taken as reference to judge the quality of a density functional. Adiabatic electron affinities (G21EA), single and double ionization potentials (G21IP and DIPCS10, respectively), and proton affinities (PA26) are

difficult test cases for density functionals suffering from SIE. Finally, SIE4 \times 4 surveys the reliability of a method in modeling the correct dissociation of cationic systems. Here, we remark again the importance of the EXX contribution in the SR region. Except for proton affinities, going from RSX-PBE ($a_x = 0$) to any other RSX hybrids ($a_x > 0$) systematically improves the performance. This improvement is especially emphasized through atomization energies for which the error decreases by $\sim 7.0 \text{ kcal mol}^{-1}$ going from RSX-PBE to RSX-PBE0. Apart from that, RSX-PBE0 and RSX-PBE0-1/3 ($a_x = 1/4$ and $a_x = 1/3$, respectively) behave similarly on these subsets, while reaching the double-hybrid class of density functionals with RSX-0DH and RSX-QIDH improves systematically the performance. In comparison, results obtained with the ω B97X-D3 ($a_x = 0.20$ and $\mu = 0.25 \text{ bohr}^{-1}$) method⁶¹ are not so predictable. The parameterized approach performs particularly well on subsets belonging to its training sets (i.e., W4-11, G21EA, and G21IP); however, it provides very large deviations for the other subsets, with a special emphasis for SIE4 \times 4.

Regarding intermolecular noncovalent interactions benchmarked on the HAL59, AHB21, CHB6, and IL16 subsets, we notice that double hybrids and ω B97X-D3 (which is empirically corrected for dispersion interactions) are in average the best approaches (Fig. 3). These density functionals decrease by a factor of 2 with respect to other RSX hybrids the binding error in halogenated

**FIG. 3.** Mean absolute deviations (kcal mol^{-1}) computed over a selection of datasets probing for basic properties and intermolecular noncovalent interactions. All computations are performed at the def2-QZVP level of theory. ω B97X-D3 related data are taken from Ref. 60.

dimers (HAL59), the MAD for RSX-PBE being $1.0 \text{ kcal mol}^{-1}$, but moderately improve intermolecular interactions involving anion-neutral, cation-neutral, and anion-cation dimers (i.e., AHB21, CHB6, and IL16). On the latter subsets, the whole fraction of EXX has a small impact on the performance. MADs lie around $2.0 \text{ kcal mol}^{-1}$ for the ion-neutral interactions (AHB21 and CHB6) and $0.5 \text{ kcal mol}^{-1}$ for the anion-cation ones (IL16). Contrary to ω B97X-D3, nonempirical RSX schemes provide an excellent estimate of anion-cation interactions (0.5 vs $1.1 \text{ kcal mol}^{-1}$) but overbind ion-neutral ones, a conclusion already pointed out in Ref. 16.

Overall, a global performance overview of each RSX approach is provided under the label TOTAL by averaging the MADs over the 10 subsets (Fig. 3). We find that upon increasing the whole fraction of EXX, more accurate results are observed. Indeed, going from $\alpha_x = 0$ to $\alpha_x = 1/3$ (RSX-PBE to RSX-PBE0-1/3, respectively), the error is decreased by $1.0 \text{ kcal mol}^{-1}$ and provides a deviation in line with ω B97X-D3 ($\alpha_x = 0.20$ and $\text{MAD} = 3.2 \text{ kcal mol}^{-1}$). RSX double hybrids, such as RSX-0DH and RSX-QIDH, bring larger performance improvements with deviations reaching 2.8 and $2.3 \text{ kcal mol}^{-1}$, respectively. As a result, we demonstrate here that by increasing the whole fraction of EXX, the performance of the RSX hybrid density functional improves. We validate also our previous assumption in the scope of the RSX scheme,⁸ which states that an increase of the hybridization scheme (i.e., switching from a global to double hybrid) improves the performance of the density functional.

As a summary, it is shown in this communication that by imposing an additional physical constraint, a reliable and fully nonempirical family of range-separated exchange hybrid density functionals is derived, casting various fractions of the whole exact-like exchange. By enforcing to reproduce the total energy of the hydrogen atom tuning the range-separation parameter, we rule in a nonempirical fashion the switch between the short- and long-range terms of the Coulomb operator. This transformation allows the recovery of the correct asymptotic behavior of the exchange potential and assures *de facto* a beneficial effect for some difficult cases for DFT like those contaminated by the spurious self-interaction error.

The derived RSX hybrids and double hybrids are benchmarked for various ground-state energy properties like ionization potentials and systems governed by covalent or noncovalent interactions especially prone to self-interaction error. We demonstrate that the resulting density functionals are very close to fulfill Koopmans' theorem by accurately estimating ionization potentials using (i) the negative value of the HOMO energy and (ii) the vertical Δ SCF approach, both approaches providing a quasiperfect linear correlation with only marginal deviations. Moreover, we find that the increase of the whole fraction of exactlike exchange in RSX hybrids often improves the performance of the density functional, especially when considering the dissociation limits of cationic molecular dimers (e.g., rare gas cations, SIE4 \times 4). Overall, we show that going from RSX hybrids to RSX double hybrids drastically improves the performance of the density functional.

Computational details: All the computations are performed with release B.01 of the Gaussian'16 program.⁶² For each energy single point, a tight SCF convergence criterion and an ultrafine integration grid are taken as a standard. The computations are done with the very large def2-QZVP Ahlrichs' quadruple- ζ basis

set⁶³ which assures a nearly complete basis set convergence and minimizes the basis set superposition error. More details about the density functionals derived in this work are reported in Table SI of the [supplementary material](#). Following the GMTKN55 benchmark recommendations,⁶⁰ electron affinities (G21EA) and anion-neutral and anion-cation interactions (AHB21 and IL16, respectively) are computed by adding diffuse *s* and *p* functions from aug-cc-pVQZ⁶⁴ to def2-QZVP, thus giving the aug-def2-QZVP basis set. The range-separation parameter μ of each nonempirical RSX models is chosen in order to reproduce the total energy of the hydrogen atom using the universal Gaussian basis set UGBS2P⁶⁵ and Hartree-Fock densities.

See [supplementary material](#) for details about the definition of the density functionals used herein and a detailed description of their performance.

E.B. thanks ANR (Agence Nationale de la Recherche) and CGI (Commissariat à l'Investissement d'Avenir) for their financial support for this work through Labex SEAM (Science and Engineering for Advanced Materials and devices) ANR 11 LABX 086, ANR 11 IDEX 05 02. The authors acknowledge the GENCI-CINES for HPC resources (Project Nos. AP010810360 and A0040810359).

REFERENCES

- W. Kohn and L. J. Sham, *Phys. Rev.* **140**, A1133 (1965).
- P. Hohenberg and W. Kohn, *Phys. Rev.* **136**, B864 (1964).
- A. D. Becke, *J. Chem. Phys.* **98**, 5648 (1993).
- A. D. Becke, *J. Chem. Phys.* **98**, 1372 (1993).
- J. Harris, *Phys. Rev. A* **29**, 1648 (1984).
- J. L. Bao, L. Gagliardi, and D. G. Truhlar, *J. Phys. Chem. Lett.* **9**, 2353 (2018).
- A. J. Cohen, P. Mori-Sánchez, and W. Yang, *Science* **321**, 792 (2008).
- E. Brémond, M. Savarese, A. J. Pérez-Jiménez, J. C. Sancho-García, and C. Adamo, *J. Phys. Chem. Lett.* **6**, 3540 (2015).
- E. Brémond, M. Savarese, N. Q. Su, A. J. Pérez-Jiménez, X. Xu, J. C. Sancho-García, and C. Adamo, *J. Chem. Theory Comput.* **12**, 459 (2016).
- H. S. Yu, S. L. Li, and D. G. Truhlar, *J. Chem. Phys.* **145**, 130901 (2016).
- A. D. Becke, *J. Chem. Phys.* **140**, 18A301 (2014).
- A. Savin, in *Recent Developments and Applications of Modern Density Functional Theory*, edited by J. M. Seminario (Elsevier, Amsterdam, 1996), pp. 327–357.
- N. Colonna, N. L. Nguyen, A. Ferretti, and N. Marzari, *J. Chem. Theory Comput.* **15**, 1905 (2019).
- J. L. Bao, Y. Wang, X. He, L. Gagliardi, and D. G. Truhlar, *J. Phys. Chem. Lett.* **8**, 5616 (2017).
- A. Dreuw and M. Head-Gordon, *J. Am. Chem. Soc.* **126**, 4007 (2004).
- M. Savarese, É. Brémond, and C. Adamo, *Theor. Chem. Acc.* **135**, 99 (2016).
- S. N. Steinmann and C. Corminboeuf, *J. Chem. Theory Comput.* **8**, 4305 (2012).
- I. Ciofini, H. Chermette, and C. Adamo, *Chem. Phys. Lett.* **380**, 12 (2003).
- J. P. Perdew and A. Zunger, *Phys. Rev. B* **23**, 5048 (1981).
- J. C. Sancho-García, Á. J. Pérez-Jiménez, M. Savarese, É. Brémond, and C. Adamo, *J. Comput. Chem.* **38**, 1509 (2017).
- M.-C. Kim, H. Park, S. Son, E. Sim, and K. Burke, *J. Phys. Chem. Lett.* **6**, 3802 (2015).
- B. G. Janesko and G. E. Scuseria, *J. Chem. Phys.* **128**, 244112 (2008).
- J. T. Margraf, P. Verma, and R. J. Bartlett, *J. Chem. Phys.* **145**, 104106 (2016).
- E. Brémond, J. C. Sancho-García, A. J. Pérez-Jiménez, and C. Adamo, *J. Chem. Phys.* **141**, 031101 (2014).
- R. K. Carlson, G. Li Manni, A. L. Sonnenberger, D. G. Truhlar, and L. Gagliardi, *J. Chem. Theory Comput.* **11**, 82 (2015).

- ²⁶G. Li Manni, R. K. Carlson, S. Luo, D. Ma, J. Olsen, D. G. Truhlar, and L. Gagliardi, *J. Chem. Theory Comput.* **10**, 3669 (2014).
- ²⁷J. Toulouse, F. Colonna, and A. Savin, *Phys. Rev. A* **70**, 062505 (2004).
- ²⁸H. Iikura, T. Tsuneda, T. Yanai, and K. Hirao, *J. Chem. Phys.* **115**, 3540 (2001).
- ²⁹T. Yanai, D. P. Tew, and N. C. Handy, *Chem. Phys. Lett.* **393**, 51 (2004).
- ³⁰J. Toulouse, W. Zhu, J. G. Ángyán, and A. Savin, *Phys. Rev. A* **82**, 032502 (2010).
- ³¹M. Wykes, N. Q. Su, X. Xu, C. Adamo, and J. C. Sancho-García, *J. Chem. Theory Comput.* **11**, 832 (2015).
- ³²M. J. G. Peach, E. I. Tellgren, P. Sałek, T. Helgaker, and D. J. Tozer, *J. Phys. Chem. A* **111**, 11930 (2007).
- ³³M. J. G. Peach, P. Benfield, T. Helgaker, and D. J. Tozer, *J. Chem. Phys.* **128**, 044118 (2008).
- ³⁴Y. Tawada, T. Tsuneda, S. Yanagisawa, T. Yanai, and K. Hirao, *J. Chem. Phys.* **120**, 8425 (2004).
- ³⁵C. Kalai and J. Toulouse, *J. Chem. Phys.* **148**, 164105 (2018).
- ³⁶A. J. Garza, I. W. Bulik, T. M. Henderson, and G. E. Scuseria, *Phys. Chem. Chem. Phys.* **17**, 22412 (2015).
- ³⁷Y. Cornaton and E. Fromager, *Int. J. Quantum Chem.* **114**, 1199 (2014).
- ³⁸Y. Cornaton, A. Stoyanova, H. J. A. Jensen, and E. Fromager, *Phys. Rev. A* **88**, 022516 (2013).
- ³⁹J.-D. Chai and M. Head-Gordon, *J. Chem. Phys.* **128**, 084106 (2008).
- ⁴⁰T. M. Henderson, A. F. Izmaylov, G. Scalmani, and G. E. Scuseria, *J. Chem. Phys.* **131**, 044108 (2009).
- ⁴¹R. Peverati and D. G. Truhlar, *J. Phys. Chem. Lett.* **2**, 2810 (2011).
- ⁴²N. Mardirossian and M. Head-Gordon, *Phys. Chem. Chem. Phys.* **16**, 9904 (2014).
- ⁴³Y. Jin and R. J. Bartlett, *J. Chem. Phys.* **145**, 034107 (2016).
- ⁴⁴R. Baer, E. Livshits, and U. Salzner, *Annu. Rev. Phys. Chem.* **61**, 85 (2010).
- ⁴⁵Z. Lin and T. Van Voorhis, *J. Chem. Theory Comput.* **15**, 1226 (2019).
- ⁴⁶L. Kronik, T. Stein, S. Refaely-Abramson, and R. Baer, *J. Chem. Theory Comput.* **8**, 1515 (2012).
- ⁴⁷T. Stein, H. Eisenberg, L. Kronik, and R. Baer, *Phys. Rev. Lett.* **105**, 266802 (2010).
- ⁴⁸I. Tamblyn, S. Refaely-Abramson, J. B. Neaton, and L. Kronik, *J. Phys. Chem. Lett.* **5**, 2734 (2014).
- ⁴⁹A. Karolewski, L. Kronik, and S. Kümmel, *J. Chem. Phys.* **138**, 204115 (2013).
- ⁵⁰É. Brémond, M. Savarese, Á. J. Pérez-Jiménez, J. C. Sancho-García, and C. Adamo, *J. Chem. Theory Comput.* **14**, 4052 (2018).
- ⁵¹J. P. Perdew, K. Burke, and M. Ernzerhof, *Phys. Rev. Lett.* **77**, 3865 (1996).
- ⁵²C. Adamo and V. Barone, *J. Chem. Phys.* **110**, 6158 (1999).
- ⁵³M. Ernzerhof and G. E. Scuseria, *J. Chem. Phys.* **110**, 5029 (1999).
- ⁵⁴C. A. Guido, E. Brémond, C. Adamo, and P. Cortona, *J. Chem. Phys.* **138**, 021104 (2013).
- ⁵⁵E. Brémond and C. Adamo, *J. Chem. Phys.* **135**, 024106 (2011).
- ⁵⁶J.-W. Song, T. Hirokawa, T. Tsuneda, and K. Hirao, *J. Chem. Phys.* **126**, 154105 (2007).
- ⁵⁷A. W. Lange, M. A. Rohrdanz, and J. M. Herbert, *J. Phys. Chem. B* **112**, 6304 (2008).
- ⁵⁸M. J. van Setten, F. Caruso, S. Sharifzadeh, X. Ren, M. Scheffler, F. Liu, J. Lischner, L. Lin, J. R. Deslippe, S. G. Louie, C. Yang, F. Weigend, J. B. Neaton, F. Evers, and P. Rinke, *J. Chem. Theory Comput.* **11**, 5665 (2015).
- ⁵⁹K. Krause, M. E. Harding, and W. Klopper, *Mol. Phys.* **113**, 1952 (2015).
- ⁶⁰L. Goerigk, A. Hansen, C. Bauer, S. Ehrlich, A. Najibi, and S. Grimme, *Phys. Chem. Chem. Phys.* **19**, 32184 (2017).
- ⁶¹Y.-S. Lin, G.-D. Li, S.-P. Mao, and J.-D. Chai, *J. Chem. Theory Comput.* **9**, 263 (2013).
- ⁶²M. J. Frisch, G. W. Trucks, H. B. Schlegel, G. E. Scuseria, M. A. Robb, J. R. Cheeseman, G. Scalmani, V. Barone, G. A. Petersson, H. Nakatsuji, X. Li, M. Caricato, A. V. Marenich, J. Bloino, B. G. Janesko, R. Gomperts, B. Mennucci, H. P. Hratchian, J. V. Ortiz, A. F. Izmaylov, J. L. Sonnenberg, D. Williams-Young, F. Ding, F. Lipparini, F. Egidi, J. Goings, B. Peng, A. Petrone, T. Henderson, D. Ranasinghe, V. G. Zakrzewski, J. Gao, N. Rega, G. Zheng, W. Liang, M. Hada, M. Ehara, K. Toyota, R. Fukuda, J. Hasegawa, M. Ishida, T. Nakajima, Y. Honda, O. Kitao, H. Nakai, T. Vreven, K. Throssell, J. A. Montgomery, Jr., J. E. Peralta, F. Ogliaro, M. J. Bearpark, J. J. Heyd, E. N. Brothers, K. N. Kudin, V. N. Staroverov, T. A. Keith, R. Kobayashi, J. Normand, K. Raghavachari, A. P. Rendell, J. C. Burant, S. S. Iyengar, J. Tomasi, M. Cossi, J. M. Millam, M. Klene, C. Adamo, R. Cammi, J. W. Ochterski, R. L. Martin, K. Morokuma, O. Farkas, J. B. Foresman, and D. J. Fox, GAUSSIAN 16 Revision B.01, Gaussian Inc., Wallingford, CT, 2016.
- ⁶³F. Weigend and R. Ahlrichs, *Phys. Chem. Chem. Phys.* **7**, 3297 (2005).
- ⁶⁴T. H. Dunning, K. A. Peterson, and D. E. Woon, *Encyclopedia of Computational Chemistry* (John Wiley & Sons, 2002).
- ⁶⁵E. V. R. de Castro and F. E. Jorge, *J. Chem. Phys.* **108**, 5225 (1998).